Published in Photonics Technology Letters (IEEE) 12, issue 12, 1610-1612, 2000
which should be used for any reference to this work

High Average Power First-Order Distributed Feedback Quantum Cascade Lasers

Daniel Hofstetter, Thierry Aellen, Mattias Beck, and Jérôme Faist, *Member, IEEE*

***Abstract*—We present distributed feedback quantum cascade lasers at 965 cm^{-1} with a high average optical output power at temperatures of up to 60 °C. At a duty cycle of 3%, the averaged maximal output power of a 55-μm wide and 1.5-mm-long device at −30 °C was 13.6 mW; at 60 °C, the device emitted 2 mW. Corresponding peak optical powers of 450 mW at −30 °C and of 70 mW at 60 °C have been observed. Due to the lateral current injection, we achieved single-mode behavior in a slightly distorted zero-order lateral mode across the whole range of investigated temperatures and output powers. At room temperature, the threshold current density was on the order of 6.7 kA/cm^2; the characteristic temperature T_0 was, due to tuning of the Bragg resonance into the gain curve, rather high, namely 310K.**

***Index Terms*—Distributed feedback laser, high average power, infrared spectroscopy, quantum cascade laser, single-mode laser.**

SINGLE-MODE quantum cascade (QC) lasers have a great application potential for infrared (IR) spectroscopy. Wavelength ranges of particular interest include those around 5 and 10 μm where, up until now, CO lasers and CO_2 lasers have been utilized for various laboratory-type experiments like photoacoustic (PA) spectroscopy, multiple-pass absorption spectroscopy [1], [2], or absorption spectroscopy in hollow waveguides and silver halide fibers [3], [4]. With the recent progresses in PA-spectroscopy, such as the advent of highly sensitive microphones and microphone arrays, the construction of resonant multi-pass PA-cells, or the deployment of Helmholtz-resonator shaped PA-cells, QC lasers are becoming very interesting light sources for this sensitive technique [5], [6]. Nevertheless, the average QC laser output power was usually not large enough to perform spectroscopy in the ppm or even the ppb range [7], [8]. It is, thus, necessary to achieve high average power under temperature conditions which can be maintained with thermo-electric coolers. This goal can be achieved mainly by operating the laser at a high duty cycle. In this letter, we report DFB lasers at 965 cm^{-1}, which emit up to 13.6-mW average power at −30 °C. Their peak wavelength is exactly at one of the strongest ammonia absorption lines and can have an immediate application for PA experiments with this particular gas.

Fabrication of these devices relied on molecular beam epitaxy (MBE) of lattice matched $In_{0.53}Ga_{0.47}As$–$In_{0.52}Al_{0.48}As$ layers on top of an n-doped InP (Si, 2×10^{17} cm^{-3}) substrate. The growth process started with the lower waveguide layers ($In_{0.53}Ga_{0.47}As$, Si, 1×10^{17} cm^{-3}, total thickness 1.5 μm), proceeded with an active region (thickness 1.75 μm) and was finished by a thicker set of upper waveguide layers ($In_{0.53}Ga_{0.47}As$, Si, 1×10^{17} cm^{-3}, thickness 2.2 μm), and a highly n-doped cap layer ($In_{0.53}Ga_{0.47}As$, Si, 1×10^{19} cm^{-3}, thickness 0.7 μm) on top. This cap layer was also the host layer for the grating, as reported earlier [7], [9]. Current injection into the grating layer was accomplished laterally through narrow metal stripes on the shoulders of the waveguide. This design has the advantages of being simple (no epitaxial re-growth), offering a strong coupling coefficient, and, finally, resulting in small absorption losses. The active region consisted of 35 periods. The laser transition was diagonal, similar as described in [10], [11]. The layer sequence of the structure, in nanometers, starting from the injection barrier, is as follows: $3.9/\mathbf{1.0}/3.8/\mathbf{1.2}/3.7/\mathbf{1.5}/3.9/\mathbf{1.7}/4.0/\mathbf{4.2}/3.1/\mathbf{0.9}/6.4/\mathbf{1.0}/6.0/\mathbf{2.8}$ nm. $In_{0.52}Al_{0.48}As$ barrier layers are in bold, $In_{0.53}Ga_{0.47}As$ well layers are in roman, and n-doped layers (Si 2.5×10^{17} cm^{-3}) are underlined.

The fabrication process started by holographically defining a grating with a 1.6378-μm period ($n_{\text{eff}} = 3.163$), and wet chemical etching of the grating to a depth of 0.3 μm in a $H_3PO_4 : H_2O_2 : H_2O$ solution (4 : 1 : 10, etch rate 800 nm/min). We used a 488-nm Ar–ion laser and a 90 ° corner reflector mounted on a rotational stage for the grating exposure. Wet chemical etching in a $HBr : HNO_3 : H_2O$ solution (1 : 1 : 10, etch rate 800 nm/min) was then used to define ridge waveguides with a width of 55 μm (etch depth 5 μm) and a length of 1.5 mm. 300 nm of Si_3N_4 served as an electrical passivation layer and Ti–Au (10/1000 nm) was used as the top contact metal. Thinning, back contacting (Ge–Au–Ag–Au, 12/27/50/100 nm), and cleaving completed the processing. No facet coatings were used; and the optical powers mentioned below are single-facet output powers. All devices were mounted ridge side up on copper heatsinks, and then placed into a Peltier-cooled aluminum box with an antireflection coated ZnSe-window. In this box, they were held at a constant temperature between −30 °C and 60 °C. A commercial pulse generator (Alpes Lasers, TPG 128) with power supply (Alpes Lasers, LDD 100) allowed us to deliver 22.5- or 45-ns-long current pulses at a variable repetition frequency of up to 5 MHz to the laser.

For spectral measurements, the light of the QC DFB laser was collected by an f/1.33 Au-coated parabolic mirror, and then bounced off a f/3.75 parabolic mirror to enter the 200-μm wide entrance slit of a grating spectrometer (Jobin–Yvon, $d_{\text{focal}} = 0.3$ m). After the spectrometer, the light was detected with a battery-driven pyro-electric detector. For the measurement of lignt output versus current (*L–I*) curves, we directly measured

The authors are with the University of Neuchâtel, Institute of Physics, CH - 2000 Neuchâtel, Switzerland (e-mail: Daniel.Hofstetter@iph.unine.ch).

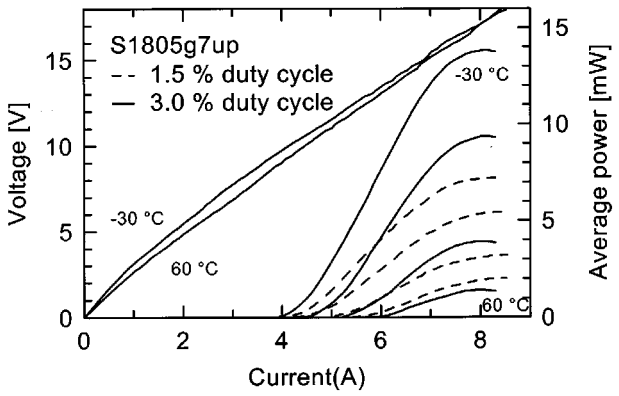

Fig. 1. Average power and voltage versus. peak current curves of a 1.5-mm-long QC DFB laser operated at both 1.5% and 3% duty cycle and at different temperatures between −30 °C and 60 °C.

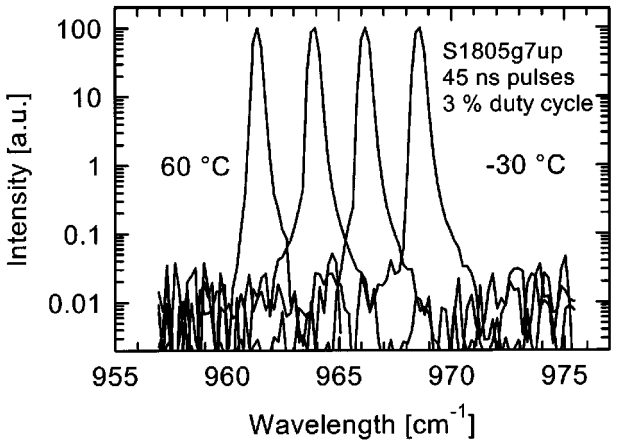

Fig. 2. Emission spectra of a 1.5-mm-long QC DFB laser operated at maximal output power for 3% duty cycle at different temperatures between −30 °C and 60°C. A pulselength of 45 ns was used for this measurement.

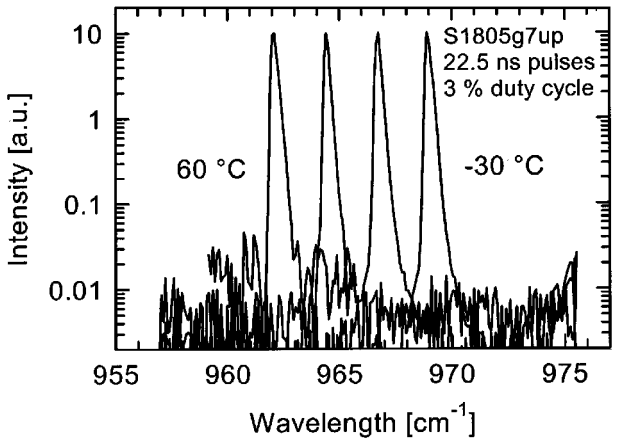

Fig. 3. Emission spectra of a 1.5-mm-long QC DFB laser operated at 3% duty cycle and with 22.5-ns-long pulses.

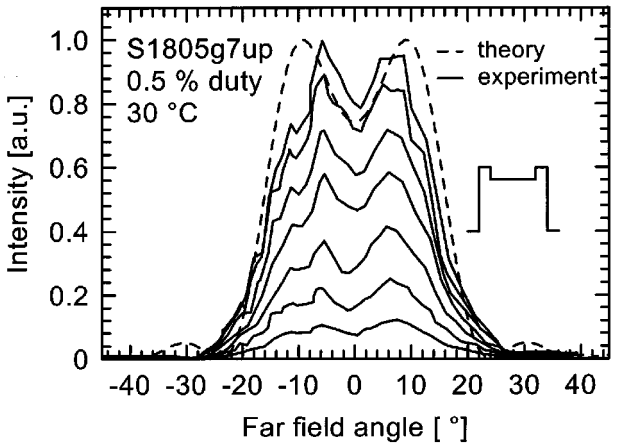

Fig. 4. Experimental (solid lines) and theoretical (dashed line) far-field distributions for a 1.5-mm-long QC DFB laser at 0.5% duty cycle and 45-ns pulselength. The measurements were taken between 4.5 and 7.5 A injection current at a temperature of −30 °C. The inset shows schematically the lateral refractive index profile used for the calculated far field.

the average power with a calibrated thermopile detector. Typical *L–I* and current versus voltage (*I–V*) curves of a 55-μm wide and 1.5-mm-long device at 1.5% duty cycle are shown in Fig. 1 (dashed lines). The emitted average power drops from 7.2 mW at −30 °C to 2 mW at 60 °C. These values correspond to peak powers of 480 and 135 mW at the respective temperatures. We observed threshold currents of 4.35 A at −30 °C and 5.8 A at 60 °C; these values are equivalent to threshold current densities of 5.3 and 7 kA/cm^2, respectively. Since the Bragg peak tuned toward the center of the gain curve at higher temperatures, we observed a relatively high T_0 of 310 K.

The solid lines of Fig. 1 show the maximal average output power measured at the same temperatures but with a doubled duty cycle of 3%. The highest output power was achieved at −30 °C; its value at the thermal roll-over point was 13.6 mW. At room temperature, we still observed 4 mW, and finally, at 60 °C, the value decreased to 1.5 mW. The last number which is smaller than the one for 1.5% duty cycle indicates that, at a temperature of 60 °C, the duty cycle with the best performance is smaller than 3%. Considering the high voltage necessary to achieve these output powers, it becomes clear that the device suffers from excessive heating, in particular at higher temperatures. This hypothesis is confirmed by Fig. 2, which shows emission spectra at maximal output power and different temperatures between −30 °C and 60 °C. A pulselength of 45 ns and a pulse repetition frequency of 667 kHz was used to drive the laser at a duty cycle of 3%. The single emission peak tunes from 968.6 cm^{-1} at −30 °C to 961.4 cm^{-1} at 60 °C. The temperature tuning is $\Delta\nu/\Delta T = -0.08$ cm^{-1}/K; a value which is 27% larger than the one we reported earlier for devices running at low duty cycle [7]. Since the temperature tuning of a DFB laser is only due to a temperature-induced refractive index change, we can use the emission wavelength as a "thermometer" for the active region. Under the assumption of a certain temperature difference ΔT between the active region and the device holder at −30 °C and using the standard temperature tuning of DFB lasers at very low duty ($\Delta\nu/\Delta T = -0.063$ cm^{-1}/K), we find at 60 °C and under 8.3-A injection current a much larger

temperature difference of $\Delta T + 25\,^{\circ}$C. At the same duty and temperature, but at 6.3 A, the corresponding temperature difference was already smaller, namely $\Delta T + 17\,^{\circ}$C. This is consistent with the observed increase in threshold current from 5.8 to 6.1 A at this temperature when going from a 1.5% to 3% duty cycle.

Constant emission peak width and side mode suppression ratio were seen for all temperatures; their respective values are 0.5 cm^{-1} and >35 dB. Fig. 3 shows the emission spectra of the same device as above driven with 22.5-ns-long current pulses at 133 MHz. Here, the full-width at half-maximum (FWHM) of the emission peaks dropped to 0.25 cm^{-1}. At the same time the output power decreased somewhat which resulted in a smaller side mode suppression of about 25 dB. Linewidth versus pulselength measurements have shown that the linewidth increased linearly with pulselength at a rate of roughly 0.01 cm^{-1}/ns.

The solid lines in Fig. 4 represent the far-field distribution of this device at seven different injection currents between 4.5 and 7.5 A. The dashed line corresponds to the calculated far field using a lateral refractive index profile with a lower index in the center of the waveguide, similar to the schematic picture shown as an inset into Fig. 4. Due to the lateral current injection and the resulting heating-induced refractive index increase at the shoulders of the waveguide, the laser emits in a slightly distorted zero-order mode. Both shape (distortion) and FWHM (30°) of the theoretical far field agree well with the far-field distributions we observed experimentally on this particular laser. It is obvious that the design with lateral current injection requires relatively large stripe widths to keep the absorption loss low. Since, in this case, the current is not correctly distributed within the 0.7-μm-thick grating layer, the probability of such a mode distortion is quite considerable.

In conclusion, we have demonstrated a single-mode QC DFB laser with an emission wavelength of 965 cm^{-1}. The device could be operated at 3% duty cycle with a maximal average output power of 13.6 mW at $-30\,^{\circ}$C. The relatively high threshold current density of 5.3 kA/cm^2 at $-30\,^{\circ}$C and 7 kA/cm^2 at 60 $^{\circ}$C led to a somewhat elevated temperature tuning coefficient of -0.08 cm^{-1}/K, compared to -0.063 cm^{-1}/K measured on earlier devices. Nevertheless, QC DFB lasers with such a high average power will be ideal light sources for mid-IR spectroscopic applications.

ACKNOWLEDGMENT

The authors would like to thank H. Bianchini and A. Müller of Alpes Lasers SA, Neuchâtel, for their technical assistance.

REFERENCES

[1] S. Bernegger and M. W. Sigrist, "CO-laser photoacoustic spectroscopy of gases and vapors for trace gas analysis," *Infrared Phys.*, vol. 30, no. 5, pp. 375–429, 1990.

[2] P. Repond, T. Marty, and M. W. Sigrist, "A continuously tunable CO_2 laser for photoacoustic detection of trace gases," *Helv. Phys. Acta*, vol. 65, no. 6, pp. 828–829, 1992.

[3] B. Mizaikoff, C. S. Murthy, M. Kraft, V. Pustogow, A. Müller, D. Hofstetter, J. Faist, and N. Croitoru, "Novel mid-infrared gas sensors based on hollow waveguides and quantum cascade lasers," in *Proc. PITTCON 2000*, New Orleans, LA, Mar. 2000.

[4] B. Mizaikoff, C. S. Murthy, M. Kraft, V. Pustogow, A. Müller, D. Hofstetter, J. Faist, S. Inberg, N. Croitoru, A. Katzir, S. Hocdé, and J. Lucas, "Quantum cascade lasers—A novel lightsource for mid-infrared sensor systems," in *Proc. 8th Int. Meeting Chemical Sensors*, Basel, Switzerland, July 2000.

[5] M. Nägele, D. Hofstetter, J. Faist, and M. W. Sigrist, "Low power quantum cascade photoacoustic spectrometer for trace-gas monitoring," in *Proc. 11th Int. Conf. Photoacoustic and Photothermal Phenomena*, Kyoto, Japan, June 25–29, 2000.

[6] R. Kästle and M. W. Sigrist, "CO-laser photoacoustic spectroscopy on the dimerization of fatty-acid molecules," *J. de Phys. 4, Colloque C7*, vol. 4, pp. 491–494, 1994.

[7] D. Hofstetter, J. Faist, A. Müller, M. Beck, and U. Oesterle, "Demonstration of high-performance 10.16 μm quantum cascade distributed feedback lasers fabricated without epitaxial re-growth," *Appl. Phys. Lett.*, vol. 75, no. 14, pp. 665–667, 1999.

[8] C. Gmachl, F. Capasso, J. Faist, A. L. Hutchinson, A. Tredicucci, D. L. Sivco, J. N. Baillargeon, S. N. G. Chu, and A. Y. Cho, "Continuous-wave and high-power pulsed operation of index-coupled distributed feedback quantum cascade laser at $\lambda \approx 8.5$ μm," *Appl. Phys. Lett.*, vol. 72, no. 12, pp. 1430–1432, 1998.

[9] D. Hofstetter, J. Faist, M. Beck, and U. Oesterle, "Surface-emitting 10.1 μm quantum cascade distributed feedback lasers," *Appl. Phys. Lett.*, vol. 75, no. 24, pp. 3769–3771, 1999.

[10] A. Müller, M. Beck, J. Faist, U. Oesterle, and M. Ilegems, "Electrically tunable, room-temperature quantum-cascade lasers," *Appl. Phys. Lett.*, vol. 75, no. 11, pp. 1509–1511, 1999.

[11] J. Faist, C. Sirtori, F. Capasso, D. L. Sivco, J. N. Baillargeon, A. L. Hutchinson, and A. Y. Cho, "High-power long-wavelength ($\lambda \approx 11.5$ μm) quantum cascade lasers operating above room temperature," *IEEE Photon. Technol. Lett.*, vol. 10, pp. 1100–1102, Aug. 1998.